Supplementary Information for

Bottom-Up Formation of the Simplest Geminal Thiol—Methanedithiol ($CH_2(SH)_2$)—and the Methyl Hydrodisulfide (H_3CSSH) Isomer in Interstellar Analog Ices

Jia Wang[1,2#], Ashanie Herath[1,2#], Andrew M. Turner[1,2], Mason McAnally[1,2], Ryan C. Fortenberry[3†], André K. Eckhardt[4‡], and Ralf I. Kaiser[1,2*]

[1] *Department of Chemistry, University of Hawai'i at Mānoa, Honolulu, HI, USA 96822*

[2] *W. M. Keck Laboratory in Astrochemistry, University of Hawai'i at Mānoa, Honolulu, HI, USA 96822*

[3] *Department of Chemistry and Biochemistry, University of Mississippi, Oxford, MS, USA 38677*

[4] *Lehrstuhl für Organische Chemie II, Ruhr-Universitat Bochum, Bochum 44801, Germany*

Corresponding authors: †r410@olemiss.edu, ‡Andre.Eckhardt@ruhr-uni-bochum.de, *ralfk@hawaii.edu

[#] *These authors contributed equally to this work*

Experimental

All experiments were carried out at the W. M. Keck Research Laboratory in Astrochemistry. The apparatus consists of a hydrocarbon-free stainless steel ultrahigh vacuum chamber operating at pressures of a few 10^{-11} Torr, maintained by magnetically suspended turbomolecular pumps backed by an oil-free scroll pump.[1,2] Inside the chamber, a polished silver substrate is mounted on a freely-rotatable cold finger cooled to 5.2 ± 0.2 K using a two-stage closed-cycle helium compressor (Sumitomo Heavy Industries, RDK-415E), as described previously.[1,3,4] Gas mixtures of hydrogen sulfide (H_2S, Sigma Aldrich, ≥ 99.5%; D_2S Sigma Aldrich, 97 atom % D) and methane (CH_4, Airgas, > 99.9%; CD_4, Sigma-Aldrich, 99.9 atom % D) with a H_2S:CH_4 ratio of 3:7 were prepared and deposited onto the polished silver substrate through a capillary array.[5] Ice growth was monitored using a helium–neon laser operating at 632.8 nm. The ice thicknesses were determined to be 1100 ± 200 nm from interference fringes in the reflected laser signal arising from thin-film interference.[6] The average refractive index of 1.37 was adopted for the mixed ice based on values of 1.41 for H_2S and 1.34 for CH_4.[7,8] The deposited ice was irradiated with energetic electrons (5 keV) at 5 K with two irradiation doses. In the high dose experiments, ices were irradiated at 100 nA for 60 minutes, corresponding to an effective dose of 7.3 ± 0.3 eV molecule^{-1} for methane and 15.6 ± 0.3 eV molecule^{-1} for hydrogen sulfide.[5] In the low dose experiments, irradiation was performed at 10 nA for 10 minutes, corresponding to doses up to 0.16 ± 0.04 eV molecule^{-1} for methane and 0.28 ± 0.04 molecule^{-1} for hydrogen sulfide to probe the isotopic mass shifts in deuterated ices.[5] Energetic electrons were generated using an electron gun (Specs PU-EQ 22). The average electrons penetration depth (400 ± 50 nm) was estimated using CASINO Monte Carlo simulations.[9] Ice thicknesses were kept significantly larger than the electron penetration depth to avoid substrate-induced chemistry. The CH_4:H_2S ratio of 0.2 ± 0.1 : 1 for the deposited ices was determined from the infrared bands and band absorption coefficients of fundamentals and combination bands of H_2S and CH_4.[5] Infrared spectra were recorded in situ using a Fourier transform infrared spectrometer (FTIR, Nicolet 6700) over the range 6000–500 cm^{-1} at a resolution of 4 cm^{-1}. FTIR measurements were performed before, during and after irradiation to monitor chemical evolution of the ice mixture. Following irradiation, the ices were warmed from 5 to 330 K at a ramp rate of 1 K min^{-1} (temperature–programmed desorption (TPD)) using a temperature programmable controller (Lake Shore 336), simulating the transformation of cold molecular clouds to star-forming regions.

During the TPD phase, subliming species were photoionized in the gas phase using tunable single-photon vacuum ultraviolet (VUV) photoionization and analyzed with a reflectron time-of-flight (ReToF) mass spectrometer (Jordan TOF Products, Inc.).[1] VUV light was produced via resonant four wave mixing schemes ($2\omega_1 \pm \omega_2$) for photons with energies of 9.34, 8.75, and 8.17 eV. VUV light was generated by spatially overlapping colinear beams of ω_1 and ω_2 in a pulsed (30 Hz) jet of rare gases. The third harmonic (355 nm) of a neodymium yttrium-aluminum garnet (Nd:YAG, Spectra-Physics, Quanta-Ray PRO 250-30) laser was utilized to generate 10.49 eV photons followed by frequency tripling in xenon. Additional photon energies (Table S2) were produced using four-wave mixing with the appropriate dye laser solutions. The generated VUV beam was spectrally isolated from other laser beams via a biconvex lithium fluoride lens (ISP Optics) in an off-axis geometry. The selected VUV photons were directed 2.0 ± 0.5 mm above the ice surface to selectively photoionize subliming molecules during TPD. The resulting ions were extracted into the ReToF-MS (Jordan TOF Products, Inc.) and detected using a microchannel plate (MCP) detector. The ion signals were amplified by a preamplifier (Ortec 9305) and recorded with a multichannel scalar (FAST ComTec, MCS6A), using a time bin width of 3.2 ns.[10,11] Each mass spectrum was obtained by integrating 3600 sweeps, corresponding to an integration time of 2 minutes.

Computational

All geometries were optimized at the CCSD(T)-F12/cc-pVTZ-F12 level of theory in MOLPRO 2025.1 program [12-16] with harmonic vibrational frequencies computed at the same level of theory. All energies are adiabatic and represent differences in the energies with the zero-point vibrational energy (ZPVE) corrections of the optimized structures included in line with previous work on related molecules.[11,17,18] The differences between the energy of the neutral structure at hand and the lowest energy isomer produce the relative energies, and the differences between the neutral and radical cation of the given isomer provide the ionization energies.

All time dependent density functional theory (TD-DFT) calculations were performed using Gaussian 16, Revision C.01.[19] The density functional theory (DFT) B3LYP functional[20,21] was employed for geometry optimizations, vibrational frequencies calculations and TD-DFT calculations, utilizing the Dunning correlation consistent split valence basis set aug-cc-pVTZ.[22]

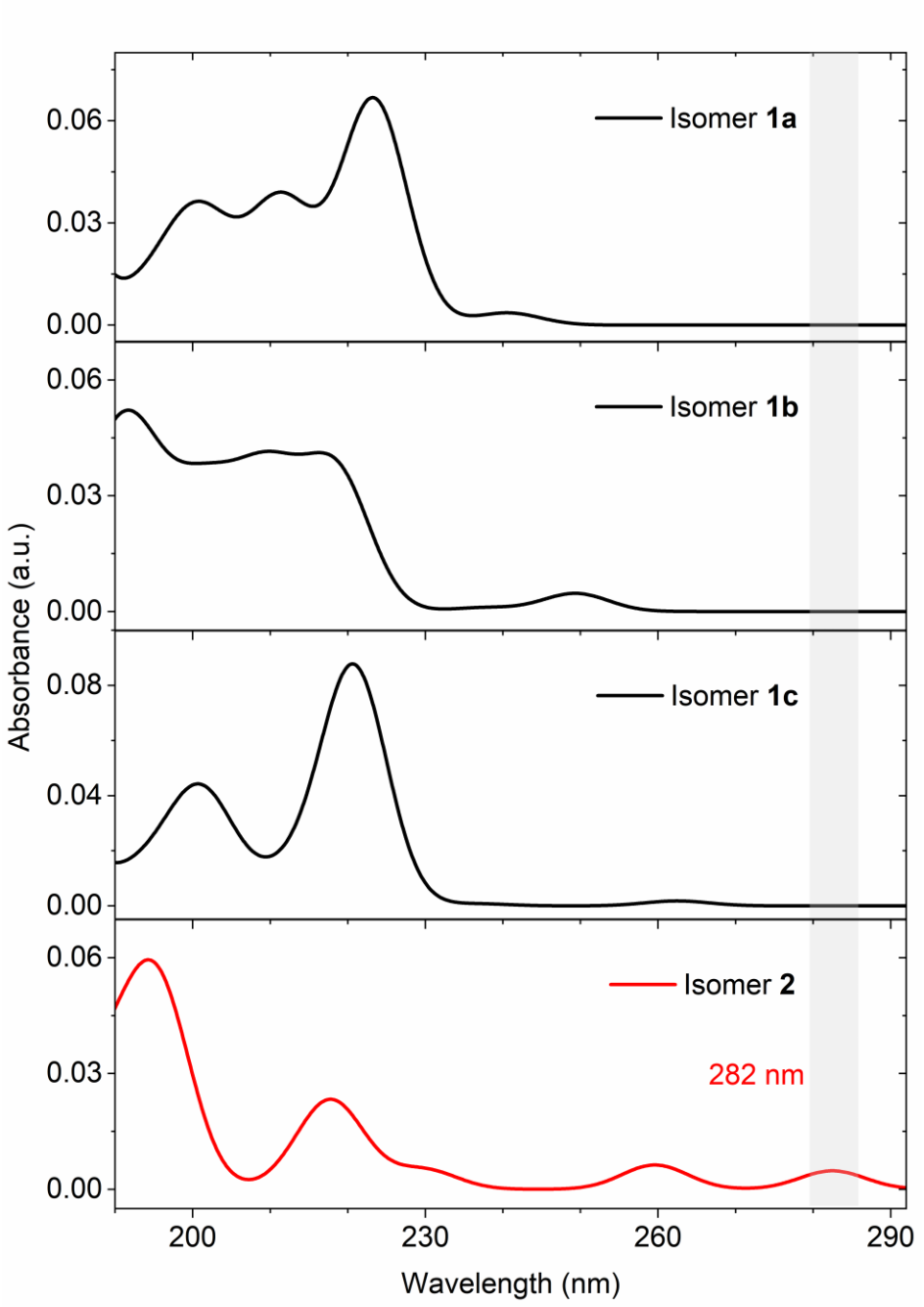

Figure S1. Simulated ultraviolet (UV) spectra of isomers **1a**, **1b**, **1c**, and **2** computed at the TD-B3LYP/aug-cc-pVTZ level of theory. The spectra were fitted with Gaussian line shape functions with a full width at half maximum (FWHM) of 20 nm.

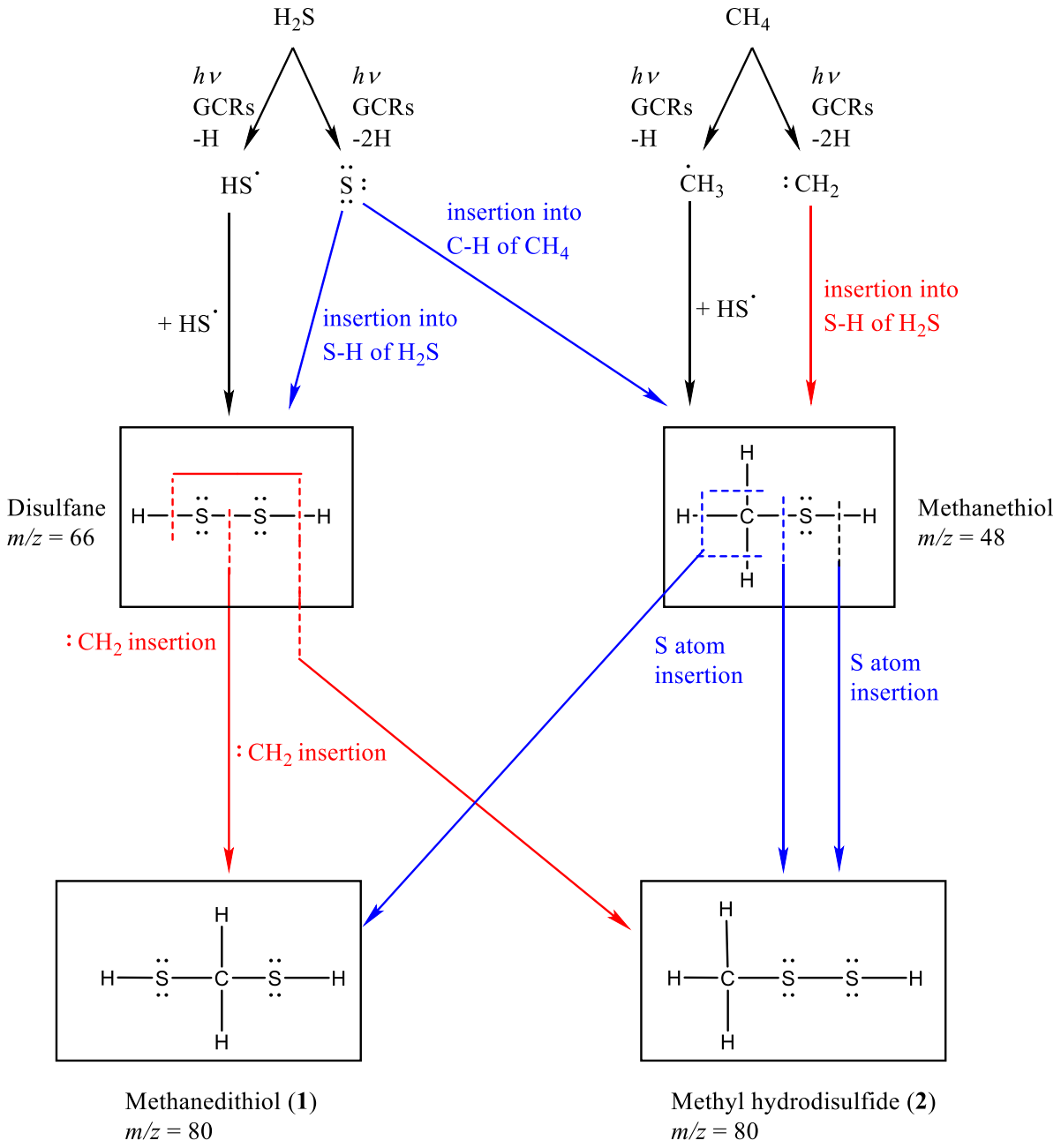

Figure S2. Proposed formation pathways of methanedithiol (**1**, $CH_2(SH)_2$) and methyl hydrodisulfide (**2**, CH_3SSH) in interstellar analog ices composed of hydrogen sulfide (H_2S) and methane (CH_4). Methanedithiol may form via S atom insertion into the C–H bond of methanethiol (CH_3SH) or methylene (CH_2) insertion into the S–S bond of disulfane (HSSH). Methyl hydrodisulfide may form via methylene insertion into the S–H bonds of disulfane or S atom insertions into C–S or S–H bonds of methanethiol. Red arrows indicate methylene insertion, and S atom insertions are indicated with blue arrows.

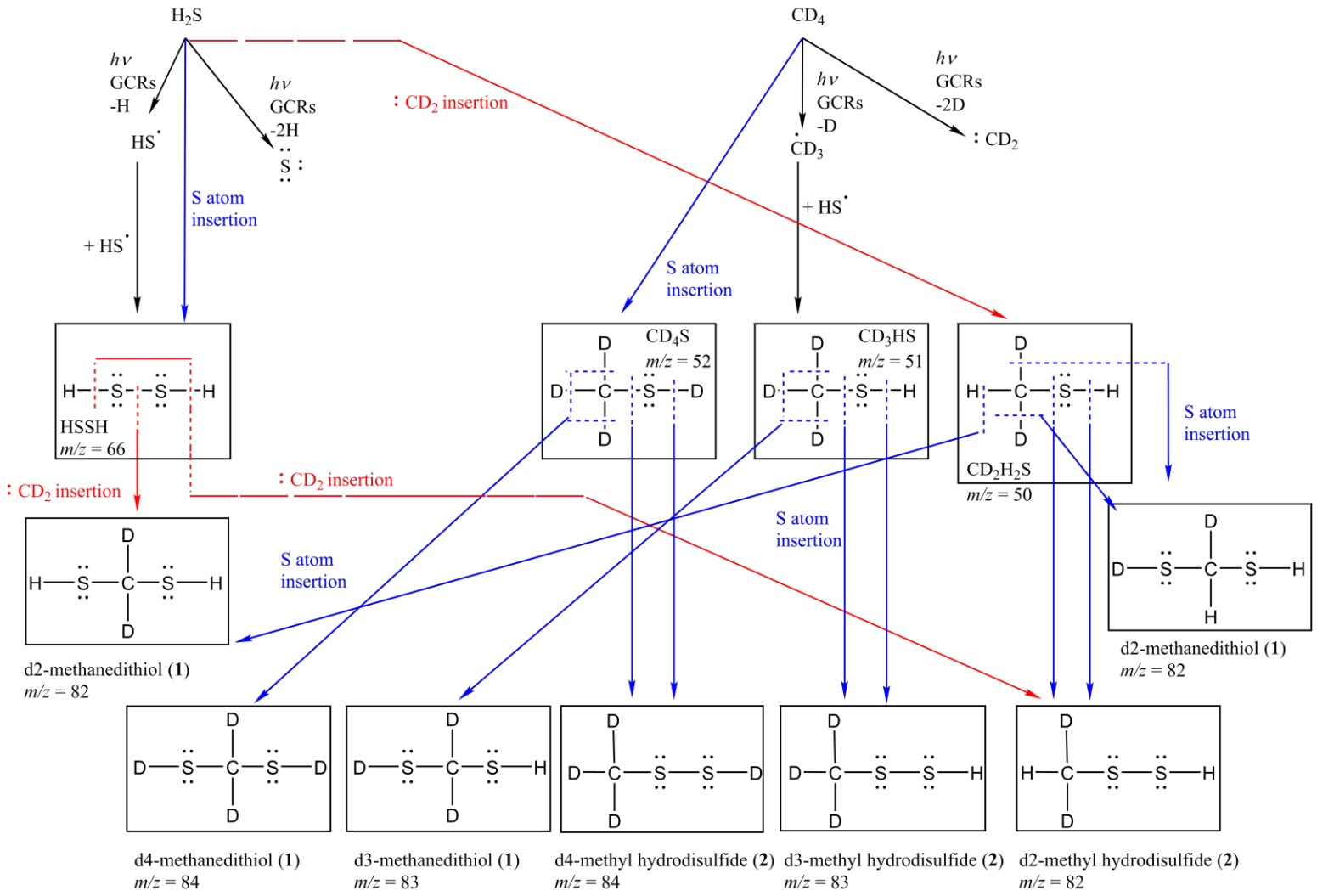

Figure S3. Proposed formation pathways of partially deuterated methanedithiol and methyl hydrodisulfide in interstellar analog ices composed of deuterated methane (CD_4) and hydrogen sulfide (H_2S). Red arrows indicate deuterated methylene (CD_2) insertions, and S atom insertions are indicated with blue arrows.

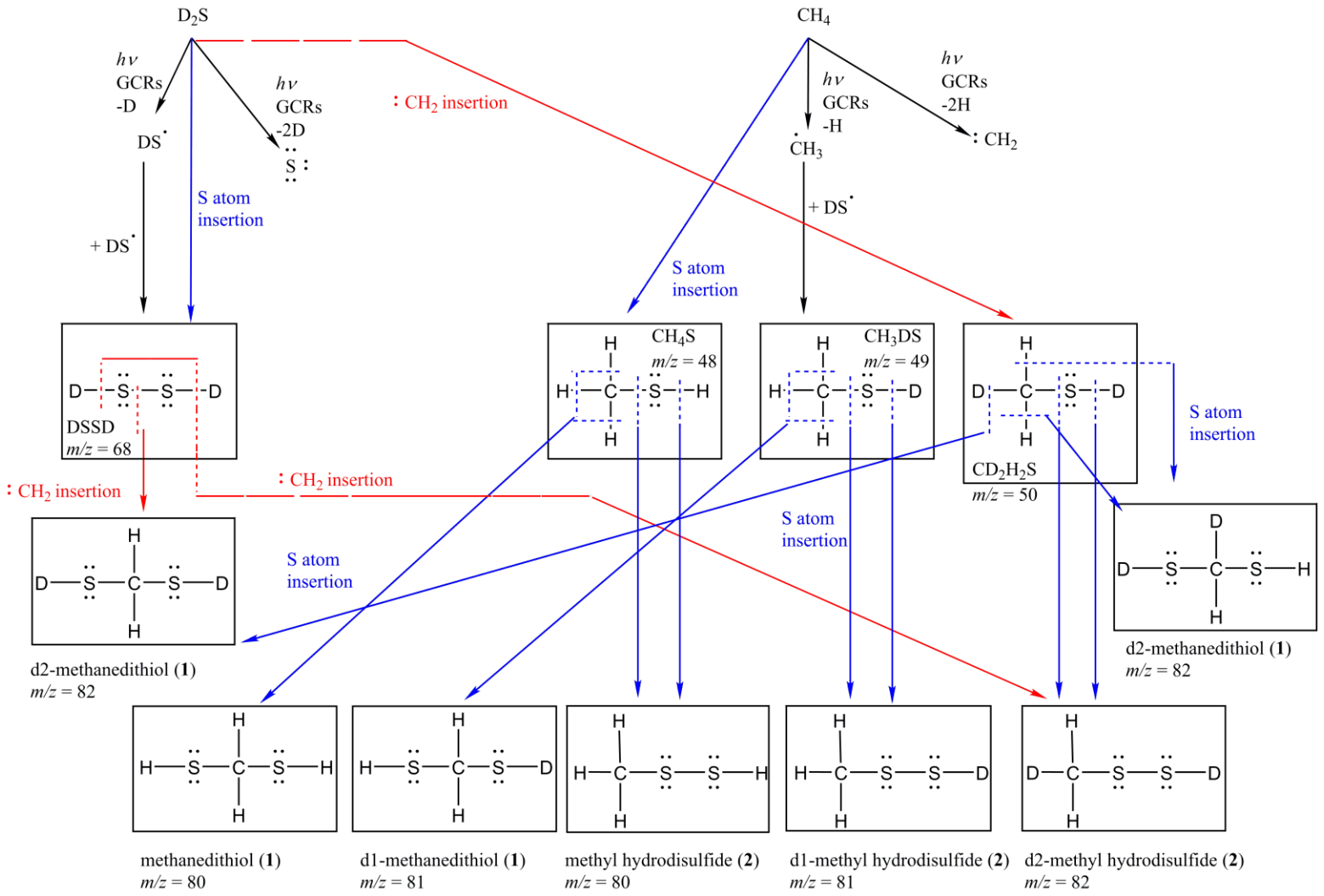

Figure S4. Proposed formation pathways of partially deuterated methanedithiol and methyl hydrodisulfide in interstellar analog ices of methane (CH_4) and deuterated hydrogen sulfide (D_2S). Red arrows indicate deuterated methylene (CH_2) insertion reactions, and S atom insertions are indicated with blue arrows.

Table S1. Uncertainty analysis of calculated adiabatic ionization energies (IEs) of CH_4S_2 isomers. All geometries are optimized at the CCSD(T)/cc-pVTZ-F12 level of theory with harmonic vibrational frequencies computed at the same level of theory. All energies are adiabatic and represent differences in the energies including the zero-point vibrational energy (ZPVE) corrections of the optimized structures. The observable IE ranges are obtained via correcting for the thermal and Stark effects by –0.03 eV and combined uncertainty limits of −0.05/+0.03 eV.[17]

	Conformer/ Isomer	Structure	Relative energy (kJ mol^{-1})	Computed IE (eV)	IE range with error (eV)	Corrected IE with Stark effect (eV)
1a	$HSCH_2SH$ (C_S)	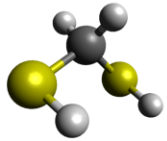	23	8.88	8.83–8.91	8.80–8.88
1b	$HSCH_2SH$ (C_1)	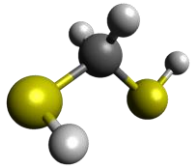	23	8.88	8.83–8.91	8.80–8.88
1c	$HSCH_2SH$ (C_2)	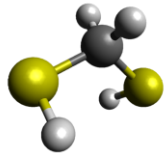	19	8.91	8.86–8.94	8.83–8.91
2	CH_3SSH (C_1)	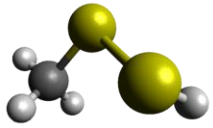	0	8.64	8.59–8.67	8.56–8.64

Table S2. Vacuum ultraviolet (VUV) photon energies used in the experiments and their generation schemes. The VUV photons was produced via resonant four-wave mixing using tunable dye lasers pumped by Nd: YAG laser(s). This configuration enables generation of photons energies with an uncertainty better than 0.001 eV.

ω_{VUV}	Medium for four-wave mixing	ω_1 (nm)	ω_2 (nm)	Photon energy (eV)
$3\omega_1$	Xenon	355	–	10.49
$2\omega_1-\omega_2$	Krypton	212.556	532	9.34
$2\omega_1-\omega_2$	Krypton	212.556	425.112	8.75
$2\omega_1-\omega_2$	Krypton	212.556	355	8.17

Table S3. Proposed molecular formulae for the ion signals observed at each mass channel in both irradiated methane–hydrogen sulfide (CH_4–H_2S) and pure hydrogen sulfide (H_2S)[23] ices. Molecules detected in the interstellar medium are indicated in bold.

m/z	CH_4–H_2S High dose				CH_4–H_2S Low dose	Proposed formula/ fragment in CH_4-H_2S ice		H_2S High dose	Proposed formula/ fragment in H_2S ice
	10.49	9.34	8.75	8.17	10.49	C-H	S-H/ C-S-H	10.49	
1	+	+	+		+		H	+	H
33	+		+		+		**SH**		
34	+				+		**H_2S**	+	H_2S
35	+				+	–		+	–
36	+				+	–		+	–
37	+				+	–		+	–
38	+				+	–		+	–
42	+					**C_3H_6 (IE = 9.73 eV)**			
46	+				+		**CH_2S**		
47	+				+		CH_3S		
48	+				+		**CH_3SH (IE = 9.439 eV)**		
49	+				+		$CH_3{}^{33}SH$		
50	+				+	**C_4H_2**	$CH_3{}^{34}SH$		
56	+					C_4H_8	**C_2S**		
59	+						C_2H_3S		
60	+	+					**C_2H_4S (CH_3CHS observed)**		
61	+	+					C_2H_5S		
62	+	+	+		+		**C_2H_6S**		
63	+	+	+				$C_2H_5{}^{34}S$		
64	+	+	+		+	C_5H_4	$C_2H_6{}^{34}S$ /S_2	+	S_2
65	+						$^{32}S^{33}S$	+	$^{32}S^{33}S$
66	+	+	+		+	C_5H_6	H_2S_2	+	H_2S_2
67	+	+			+		$H_2{}^{33}S^{32}S$	+	$H_2{}^{33}S^{32}S$

68	+	+			+	C_5H_8	$H_2{}^{34}S^{32}S$	+	$H_2{}^{34}S^{32}S$
69	+				+		$H_2{}^{33}S^{34}S$	+	$H_2{}^{33}S^{34}S$
70	+				+	C_5H_{10}	$H_2{}^{34}S_2$	+	$H_2{}^{34}S_2$
74	+	+	+				C_3H_6S		
75	+	+					C_3H_7S		
76	+	+	+			C_6H_4	**CS_2 (IE = 10.073 ± 0.005 eV)**/ C_3H_8S		
77	+	+	+				CHS_2		
78	+	+	+			**C_6H_6**	**CH_2S_2**		
79	+	+					CH_3S_2		
80	+	+	+		+	C_6H_8	CH_4S_2		
81	+	+			+		$CH_4{}^{33}S^{32}S$		
82	+	+			+	C_6H_{10}	C_4H_2S/ $C_4{}^{34}S$/ $CH_4{}^{34}S^{32}S$		
83	+						C_4H_3S/ $CH_4{}^{34}S^{33}S$		
84	+					C_6H_{12}	C_4H_4S/ $CH_4{}^{34}S_2$		
85	+					C_6H_{13}			
86	+					C_6H_{14}			
87	+						C_4H_7S		
88	+	+	+				C_4H_8S		
89	+	+					C_4H_9S		
90	+	+	+			C_7H_6	$C_4H_{10}S$		
91	+						$C_2H_3S_2$		
92	+	+				C_7H_8	$C_2H_4S_2$		
93	+	+	+				$C_2H_5S_2$		
94	+	+	+		+	C_7H_{10}	$C_2H_6S_2$		
95	+	+	+				$C_2H_6{}^{33}S^{32}S$		
96	+	+	+		+	C_7H_{12}	$C_2H_6{}^{34}S^{32}S$ /S_3	+	S_3
97	+						$^{33}S^{32}S_2$	+	$^{33}S^{32}S_2$
98	+	+	+		+	C_7H_{14}	H_2S_3	+	H_2S_3
99	+	+			+		$H_2{}^{33}S^{32}S_2$	+	$H_2{}^{33}S^{32}S_2$
100	+	+				C_7H_{16}	$H_2{}^{34}S^{32}S_2$	+	$H_2{}^{34}S^{32}S_2$

101	+						$H_2{}^{33}S^{34}S^{32}S$	+	$H_2{}^{33}S^{34}S^{32}S$
102	+		+				$H_2{}^{32}S^{34}S_2$	+	$H_2{}^{32}S^{34}S_2$
103	+						$C_3H_3S_2/C_5H_{11}S$		
104	+					C_8H_8	$C_3H_4S_2/C_5H_{12}S$		
105	+						$C_3H_5S_2$		
106	+	+	+			C_8H_{10}	$C_3H_6S_2$		
107	+	+	+				C_6H_3S /$C_3H_7S_2$		
108	+	+	+			C_8H_{12}	$C_3H_8S_2$		
110	+	+	+			C_8H_{14}	C_6H_6S/ CH_2S_3		
111	+	+					CH_3S_3		
112	+	+	+		+	C_8H_{16}	CH_4S_3		
113	+	+					$CH_4S_2{}^{33}S$		
114	+	+			+	C_8H_{18}	$C_6H_{10}S$/ $CH_4S_2{}^{34}S$		
115	+	+					$C_6H_{11}S$		
116	+	+					$C_6H_{12}S$/ $CH_4S^{34}S_2$		
122	+	+	+			C_9H_{14}	$C_4H_{10}S_2$/ $C_2H_2S_3$		
123	+	+					$C_2H_3S_3$		
124	+	+				C_9H_{16}	$C_2H_4S_3$		
125	+	+	+				$C_2H_5S_3$		
126	+	+	+			C_9H_{18}	$C_2H_6S_3$		
127	+	+	+				$C_2H_6{}^{33}S^{32}S_2$		
128	+	+	+		+	C_9H_{20}	S_4	+	S_4
129	+						$^{33}S^{32}S_3$	+	$^{33}S^{32}S_3$
130	+	+	+		+		H_2S_4	+	H_2S_4
131	+	+			+		$H_2{}^{33}S^{32}S_3$	+	$H_2{}^{33}S^{32}S_3$
132	+	+			+	C_9H_{10}	$H_2{}^{34}S^{32}S_3$	+	$H_2{}^{34}S^{32}S_3$
133	+	+			+		$H_2{}^{34}S^{33}S^{32}S_2$	+	$H_2{}^{34}S^{33}S^{32}S_2$
134	+	+			+	$C_{10}H_{14}$	$H_2{}^{34}S_2{}^{32}S_2$	+	$H_2{}^{34}S_2{}^{32}S_2$
138	+	+	+			$C_{10}H_{18}$	$C_3H_6S_3$		
139	+	+	+				$C_3H_7S_3$		

140	+	+	+			$C_{10}H_{20}$	$C_3H_8S_3$		
141	+	+					CHS_4		
142	+	+	+			$C_{10}H_{22}$	$C_6H_6S_2$ / CH_2S_4		
143	+	+					CH_3S_4		
144	+	+	+		+		CH_4S_4		
145	+	+	+				$CH_4S_3{}^{33}S$		
146	+	+	+		+		$CH_4S_3{}^{34}S$		
147	+	+					$CH_4S_2{}^{34}S^{33}S$		
148	+	+					$CH_4S_2{}^{34}S_2$		
149	+	+	+	+			$C_6H_{13}S_2$		
152						$C_{11}H_{20}$		+	-
153								+	-
154	+	+	+			$C_{11}H_{22}$	$C_2H_3S_4$/ $C_4H_{10}S_3$	+	-
155	+						$C_2H_3S_4$	+	-
156	+	+				$C_{11}H_{24}$	$C_2H_4S_4$	+	-
157	+	+	+				$C_2H_5S_4$	+	-
158	+	+	+		+		$C_2H_6S_4$	+	-
159	+	+	+				$C_2H_6{}^{33}S^{32}S_3$		
160	+	+	+		+		$C_2H_6{}^{34}S^{32}S_3$/S_5	+	S_5
161	+	+					$^{33}S^{32}S_4$	+	$^{33}S^{32}S_4$
162	+	+	+		+	$C_{12}H_{18}$	H_2S_5	+	H_2S_5
163	+	+					$H_2{}^{33}S^{32}S_4$	+	$H_2{}^{33}S^{32}S_4$
164	+	+				$C_{12}H_{20}$	$H_2{}^{34}S^{32}S_4$	+	$H_2{}^{34}S^{32}S_4$
165	+	+					$H_2{}^{34}S^{33}S^{32}S_3$	+	$H_2{}^{34}S^{33}S^{32}S_3$
166	+	+				$C_{12}H_{22}$	$H_2{}^{34}S_2{}^{32}S_3$	+	$H_2{}^{34}S_2{}^{32}S_3$
172	+	+	+				$C_3H_8S_4$		
173	+		+				$C_3H_8{}^{33}S^{32}S_3$		
174	+	+	+				$C_3H_8{}^{34}S^{32}S_3$/$C_6H_6S_3$		
175	+	+					CH_3S_5		
176	+	+	+		+		CH_4S_5		
177	+	+	+				$CH_3{}^{34}S^{32}S_4$/ $CH_4{}^{33}S^{32}S_4$		

178	+	+	+				$CH_4{}^{34}S^{32}S_4$		
179	+	+	+				$CH_4{}^{34}S^{33}S^{32}S_3$		
180	+	+	+				$CH_4{}^{34}S_2{}^{32}S_3$		
186	+	+	+				$C_2H_3S_5$		
188	+	+					$C_2H_4S_5$		
189	+	+	+				$C_2H_5S_5$		
190	+	+	+				$C_2H_6S_5$		
191	+	+	+				$C_2H_5{}^{34}S^{32}S_4/C_2H_6{}^{33}S^{32}S_4$		
192	+	+	+		+	$C_{14}H_{24}$	S_6	+	S_6
193	+	+					$^{33}S^{32}S_5$	+	$^{33}S^{32}S_5$
194	+	+	+			$C_{14}H_{24}$	$^{34}S^{32}S_5/H_2S_6$	+	$^{34}S^{32}S_5/H_2S_6$
195	+	+					$H_2{}^{33}S^{32}S_5$	+	$H_2{}^{33}S^{32}S_5$
196	+	+	+			$C_{14}H_{28}$	$H_2{}^{34}S^{32}S_5$	+	$H_2{}^{34}S^{32}S_5$
198	+						$H_2{}^{34}S_2{}^{32}S_4$	+	$H_2{}^{34}S_2{}^{32}S_4$
204	+	+	+				$C_3H_8S_5$		
206	+	+	+				$CH_2S_6/C_6H_6S_4$		
207	+	+	+				CH_3S_6		
208	+	+	+				CH_4S_6		
209	+	+	+				$CH_5S_6/CH_4{}^{33}S^{32}S_5$		
210	+	+					$CH_4{}^{34}S^{32}S_5/C_6H_{10}S_4$		
222	+	+	+			$C_{16}H_{30}$	$C_2H_6S_6$		
224	+	+	+			$C_{16}H_{32}$	$C_2H_6{}^{34}S^{32}S_5/S_7$	+	S_7
225	+	+					$^{33}S^{32}S_6$	+	$^{33}S^{32}S_6$
226	+	+	+				$^{34}S^{32}S_6/H_2S_7$	+	$^{34}S^{32}S_6/H_2S_7$
227	+	+					$H_2{}^{33}S^{32}S_6$	+	$H_2{}^{33}S^{32}S_6$
228	+	+	+				$H_2{}^{34}S^{32}S_6$	+	$H_2{}^{34}S^{32}S_6$
230								+	$H_2{}^{34}S_2{}^{32}S_5$
236	+	+	+				$C_3H_8S_6$		
238	+	+	+				$CH_2S_7/C_6H_6S_5$		
239	+	+	+				CH_3S_7		
240	+	+	+				CH_4S_7		

241	+	+	+				$CH_3{}^{34}S^{32}S_6$		
242	+	+	+				$CH_4{}^{34}S^{32}S_6$		
254	+	+	+				$C_2H_6S_7$		
256	+	+	+		+		S_8	+	S_8
257	+	+					$^{33}S^{32}S_7$	+	$^{33}S^{32}S_7$
258	+	+	+		+		$^{34}S^{32}S_7$/ H_2S_8	+	$^{34}S^{32}S_7$/ H_2S_8
259	+	+					$H_2{}^{33}S^{32}S_7$	+	$H_2{}^{33}S^{32}S_7$
260	+	+	+				$H_2{}^{34}S^{32}S_7$	+	$H_2{}^{34}S^{32}S_7$
261	+	+					$H_2{}^{34}S^{33}S^{32}S_6$	+	$H_2{}^{34}S^{33}S^{32}S_6$
262	+	+					$H_2{}^{34}S_2{}^{32}S_6$	+	$H_2{}^{34}S_2{}^{32}S_6$
268			+				$C_3H_8S_7$		
270	+	+	+				CH_2S_8		
271	+	+	+				CH_3S_8		
272							CH_4S_8		
286		+	+				$C_2H_6S_8$		
288	+	+	+				S_9	+	S_9
290	+	+	+				H_2S_9	+	H_2S_9
292	+	+					$H_2{}^{34}S^{32}S_8$	+	$H_2{}^{34}S^{32}S_8$
320	+						S_{10}	+	S_{10}

Table S4. Cartesian coordinates (Å) of structures of CH_4S_2 isomers optimized at the CCSD(T)/cc-pVTZ-F12 level of theory and harmonic vibrational frequencies (cm^{-1}). Only one conformer of the geminal dithiol cation exists, the **1c** form.

1a CCSD(T)-F12/CC-PVTZ-F12

C	0.1033210280	0.7739872000	0.0000000000
H	-0.7240750266	1.4828075612	0.0000000000
H	1.0305680968	1.3404645162	0.0000000000
S	-0.0579094565	-0.1621462908	-1.5421504178
S	-0.0579094565	-0.1621462908	1.5421504178
H	1.0730990233	-0.8657404976	-1.4016433410
H	1.0730990233	-0.8657404976	1.4016433410

1b CCSD(T)-F12/CC-PVTZ-F12

C	0.8360719667	0.0315851116	-0.0016367654
H	1.4493530809	0.9288612107	0.0031939649
H	1.4776932290	-0.8469709852	-0.0398877305
S	-0.1705504516	-0.0376596085	-1.4992613315
S	-0.2325104247	-0.0187038179	1.4673287577
H	-0.8065205962	1.1243692078	-1.2954407910
H	0.7368579618	0.2101370523	2.3673325907

1c$^+$ CCSD(T)-F12/CC-PVTZ-F12

C	0.0000000000	0.0000000000	1.0048188144
H	-0.0101392902	0.9028080049	1.6076504539
H	0.0101392902	-0.9028080049	1.6076504539
S	1.3232735124	-0.0393396036	-0.2230707693
S	-1.3232735124	0.0393396036	-0.2230707693
H	1.3027641851	1.2780179099	-0.4992417456
H	-1.3027641851	-1.2780179099	-0.4992417456

1c CCSD(T)-F12/CC-PVTZ-F12

C	0.0000000000	0.0000000000	0.7967414642
H	-0.0374166797	0.8811252321	1.4348576268
H	0.0374166797	-0.8811252321	1.4348576268
S	1.5323472599	-0.0270102423	-0.1663810247
S	-1.5323472599	0.0270102423	-0.1663810247
H	1.2634870348	1.0680359164	-0.8898402757
H	-1.2634870348	-1.0680359164	-0.8898402757

2 CCSD(T)-F12/CC-PVTZ-F12

C	0.0022010602	-0.8052115786	1.6443466517
H	0.2312857281	-0.4404914787	2.6464274708
S	-0.0074227202	0.6390614671	0.5538985518
S	0.0452254253	-0.2230821824	-1.2998837490
H	-0.9662738847	-1.3011632347	1.6435829683
H	0.7808019864	-1.4970335202	1.3301452468
H	-1.2744501163	-0.3973412860	-1.4869356630

2$^+$ CCSD(T)-F12/CC-PVTZ-F12

C	-0.0000002739	-0.7575400390	1.6726530123
H	-0.0000377311	-0.2839786398	2.6544370823
S	0.0000010120	0.6265355478	0.5170904243
S	-0.0000008621	-0.2022041718	-1.2952201573
H	-0.9048741083	-1.3464227576	1.5303637530
H	0.9048906965	-1.3464086624	1.5304142347
H	0.0000196383	-1.4929505454	-0.8968688288

1a Wavenumbers [cm^{-1}]

208.73	230.24	275.20	661.30	770.89
783.32	940.72	989.90	1170.90	1249.86
1468.82	2684.72	2703.21	3079.64	3143.26

1b Wavenumbers [cm^{-1}]

167.38	219.93	294.92	641.43	732.12
771.78	867.18	1058.46	1206.61	1260.86
1448.95	2705.60	2707.71	3084.31	3146.37

1c$^+$ Wavenumbers [cm^{-1}]

274.86	401.57	428.91	648.78	750.16
763.00	876.27	1046.41	1149.13	1205.96
1440.34	2670.92	2671.53	3117.82	3209.22

1c Wavenumbers [cm^{-1}]

217.62	239.77	297.12	650.83	719.33
783.72	915.03	1012.75	1208.38	1264.11
1460.32	2706.72	2707.10	3077.98	3137.35

2$^+$ Wavenumbers [cm^{-1}]

133.96	248.02	254.94	588.10	692.28
883.72	942.25	998.91	1351.53	1451.90
1453.18	2632.14	3043.26	3157.33	3162.80

2 Wavenumbers [cm^{-1}]

159.65	248.26	331.47	525.26	720.15
896.77	975.12	983.13	1352.40	1466.39
1485.23	2656.01	3042.99	3136.85	3149.00

Table S5. Simulated ultraviolet (UV) spectra. Wavelengths (nm) and intensities (km mol^{-1}) are calculated at the TD-B3LYP/aug-cc-pVTZ level of theory.

1a

Wavelengths (nm)	Oscillator strength
240.58	0.0036
223.33	0.0661
211.4	0.0362
205.66	0.0003
200.89	0.0312
195.38	0.001
194.75	0.0079
193.3	0.0005
187.34	0.002
182.2	0.0089
179.8	0.0943
175.97	0.0086
168.86	0.0178
166.34	0.0005
165.31	0.0222

1b

Wavelengths (nm)	Oscillator strength
249.35	0.0047
237.54	0.001
218.7	0.0342
211.09	0.0213
207.5	0.0167
200.83	0.0196
200.76	0.008
192.37	0.0117
191.63	0.0327
186.34	0.0078
184.65	0.0061
179.03	0.009
169.08	0.0015
165.51	0.013
162.51	0.0368
162	0.0173

1c

Wavelengths (nm)	Oscillator strength
262.45	0.0018
236.48	0.0008
220.74	0.0864
212.06	0.0109
201.77	0.0205
200.53	0.0201
196.42	0.0043
194.09	0.0024
191.65	0.0071
183.32	0.0027
180.88	0.0338
178.9	0.0215
176.21	0.006
172.36	0.0251
165.51	0.0525
164.2	0.0098

2

Wavelengths (nm)	Oscillator strength
282.48	0.0048
259.59	0.0063
229.79	0.0051
218.01	0.0213
214.64	0.0026
195.79	0.0288
194.97	0.0227
188.77	0.0228
184.15	0.0018
181.1	0.0136
176.99	0.0167
174.88	0.0048
172.99	0.0118
169.44	0.1076
167.14	0.0314
166.81	0.0895

Supplementary References

(1) Abplanalp, M. J.; Forstel, M.; Kaiser, R. I. Exploiting single photon vacuum ultraviolet photoionization to unravel the synthesis of complex organic molecules in interstellar ices. *Chem. Phys. Lett.* **2016**, *644*, 79-98.
(2) Wang, J.; Zhang, C.; Marks, J. H.; Evseev, M. M.; Kuznetsov, O. V.; Antonov, I. O.; Kaiser, R. I. Interstellar formation of lactaldehyde, a key intermediate in the methylglyoxal pathway. *Nat. Commun.* **2024**, *15*, 10189.
(3) Turner, A. M.; Kaiser, R. I. Exploiting photoionization reflectron time-of-flight mass spectrometry to explore molecular mass growth processes to complex organic molecules in interstellar and solar system ice analogs. *Acc. Chem. Res.* **2020**, *53*, 2791-2805.
(4) Jones, B. M.; Kaiser, R. I. Application of reflectron time-of-flight mass spectroscopy in the analysis of astrophysically relevant ices exposed to ionization radiation: Methane (CH_4) and D4-methane (CD_4) as a case study. *J. Phys. Chem. Lett.* **2013**, *4*, 1965-1971.
(5) Herath, A.; Turner, A. M.; McAnally, M.; Wang, J.; Kaiser, R. I. Formation of dimethyl sulfide (CH_3SCH_3) and ethanethiol (CH_3CH_2SH) in interstellar analog ices of methane (CH_4) and hydrogen sulfide (H_2S). *Phys. Chem. Chem. Phys.* **2026**, *28*, 5094-5110.
(6) Turner, A. M.; Abplanalp, M. J.; Chen, S. Y.; Chen, Y. T.; Chang, A. H. H.; Kaiser, R. I. A photoionization mass spectroscopic study on the formation of phosphanes in low temperature phosphine ices. *Phys. Chem. Chem. Phys.* **2015**, *17*, 27281-27291.
(7) Hudson, R. L.; Gerakines, P. A. Infrared spectra and interstellar sulfur: New laboratory results for H_2S and four malodorous thiol ices. *Astrophys. J.* **2018**, *867*, 138.
(8) Turner, A. M.; Abplanalp, M. J.; Blair, T. J.; Dayuha, R.; Kaiser, R. I. An infrared spectroscopic study toward the formation of alkylphosphonic acids and their precursors in extraterrestrial environments. *Astrophys. J., Suppl. Ser.* **2018**, *234*, 6.
(9) Drouin, D.; Couture, A. R.; Joly, D.; Tastet, X.; Aimez, V.; Gauvin, R. CASINO V2.42 - A fast and easy-to-use modeling tool for scanning electron microscopy and microanalysis users. *Scanning* **2007**, *29*, 92-101.
(10) Kleimeier, N. F.; Turner, A. M.; Fortenberry, R. C.; Kaiser, R. I. On the formation of the popcorn flavorant 2,3-Butanedione ($CH_3COCOCH_3$) in acetaldehyde-containing interstellar ices. *ChemPhysChem* **2020**, *21*, 1531-1540.
(11) Marks, J. H.; Wang, J.; Fortenberry, R. C.; Kaiser, R. I. Preparation of methanediamine ($CH_2(NH_2)_2$—A precursor to nucleobases in the interstellar medium. *Proc. Natl. Acad. Sci. U.S.A.* **2022**, *119*, e2217329119.
(12) Adler, T. B.; Knizia, G.; Werner, H.-J. A simple and efficient CCSD(T)-F12 approximation. *J. Chem. Phys.* **2007**, *127*, 221106.
(13) Knizia, G.; Adler, T. B.; Werner, H.-J. Simplified CCSD(T)-F12 methods: Theory and benchmarks. *J. Chem. Phys.* **2009**, *130*, 054104.
(14) Raghavachari, K.; Trucks, G. W.; Pople, J. A.; Head-Gordon, M. A fifth-order perturbation comparison of electron correlation theories. *Chem. Phys. Lett.* **1989**, *157*, 479-483.
(15) Peterson, K. A.; Adler, T. B.; Werner, H.-J. Systematically convergent basis sets for explicitly correlated wavefunctions: The atoms H, He, B–Ne, and Al–Ar. *J. Chem. Phys.* **2008**, *128*, 084102.
(16) Werner, H.; Knowles, P.; Knizia, G.; Manby, F.; Schütz, M.; Celani, P.; Györffy, W.; Kats, D.; Korona, T.; Lindh, R. MOLPRO, version 2025.1, a package of ab initio programs; *see* http://www.molpro.net **2025**.

(17) Zhu, C.; Kleimeier, N. F.; Turner, A. M.; Singh, S. K.; Fortenberry, R. C.; Kaiser, R. I. Synthesis of methanediol [$CH_2(OH)_2$]: The simplest geminal diol. *Proc. Natl. Acad. Sci. U.S.A.* **2022**, *119*, e2111938119.
(18) Singh, S. K.; Zhu, C.; La Jeunesse, J.; Fortenberry, R. C.; Kaiser, R. I. Experimental identification of aminomethanol (NH_2CH_2OH)—The key intermediate in the Strecker Synthesis. *Nat. Commun.* **2022**, *13*, 375.
(19) M. J. Frisch, G. W. T., H. B. Schlegel, G. E. Scuseria, M. A. Robb, J. R. Cheeseman, G. Scalmani, V. Barone, G. A. Petersson, H. Nakatsuji, X. Li, M. Caricato, A. V. Marenich, J. Bloino, B. G. Janesko, R. Gomperts, B. Mennucci, H. P. Hratchian, J. V. Ortiz, A. F. Izmaylov, J. L. Sonnenberg, D. Williams-Young, F. Ding, F. Lipparini, F. Egidi, J. Goings, B. Peng, A. Petrone, T. Henderson, D. Ranasinghe, V. G. Zakrzewski, J. Gao, N. Rega, G. Zheng, W. Liang, M. Hada, M. Ehara, K. Toyota, R. Fukuda, J. Hasegawa, M. Ishida, T. Nakajima, Y. Honda, O. Kitao, H. Nakai, T. Vreven, K. Throssell, J. A. Montgomery, Jr., J. E. Peralta, F. Ogliaro, M. J. Bearpark, J. J. Heyd, E. N. Brothers, K. N. Kudin, V. N. Staroverov, T. A. Keith, R. Kobayashi, J. Normand, K. Raghavachari, A. P. Rendell, J. C. Burant, S. S. Iyengar, J. Tomasi, M. Cossi, J. M. Millam, M. Klene, C. Adamo, R. Cammi, J. W. Ochterski, R. L. Martin, K. Morokuma, O. Farkas, J. B. Foresman, D. J. Fox. Gaussian 16 Rev. C.01. Gaussian Inc. Wallingford, CT: 2016.
(20) Becke, A. D. Density-functional thermochemistry. III. The role of exact exchange. *J. Chem. Phys.* **1993**, *98*, 5648-5652.
(21) Becke, A. D. Density-functional exchange-energy approximation with correct asymptotic behavior. *Phys. Rev. A* **1988**, *38*, 3098-3100.
(22) Dunning, T. H. Gaussian basis sets for use in correlated molecular calculations. I. The atoms boron through neon and hydrogen. *J. Chem. Phys.* **1989**, *90*, 1007-1023.
(23) Herath, A.; McAnally, M.; Turner, A. M.; Wang, J.; Marks, J. H.; Fortenberry, R. C.; Garcia-Alvarez, J. C.; Gozem, S.; Kaiser, R. I. Missing interstellar sulfur in inventories of polysulfanes and molecular octasulfur crowns. *Nat. Commun.* **2025**, *16*, 5571.